

*Full Length Research Paper*

# Entropy generation in convection over an inclined backward-facing step with bleeding

S. A. Gandjalikhan Nassab<sup>1\*</sup>, A. Bahrami<sup>1</sup> and R. Moosavi<sup>2</sup>

<sup>1</sup>Mechanical Engineering Department, Shahid Bahonar University, Kerman, Iran.

<sup>2</sup>Mechanical Engineering Department, Yasouj University, Yasouj, Iran.

Accepted 18 May, 2011

The current work investigates entropy generation around an inclined backward-facing step under bleeding conditions using suction/blowing. The entropy generation is due to heat transfer and fluid flow in forced convection laminar flow in a duct with inclined step. The set of governing equations containing conservations of mass, momentum and energy are solved numerically to calculate the velocity and temperature profiles inside the flow domain. Because of the complex flow geometry, conformal mapping is used to generate an orthogonal grid by means of the Schwarz-Christoffel transformation. The governing equations are transformed into the computational domain and the discretized forms of the governing equations are obtained by the control volume method. In the numerical computations, the SIMPLE algorithm is used for the pressure-velocity coupling. Numerical expressions, in terms of entropy generation number (Ns), Bejan number (Be) and Nusselt number (Nu) are derived in dimensionless forms using velocity and temperature profiles. The effects of step inclined angle and bleed coefficient on the entropy generation number, Nusselt number, Bejan number and friction coefficient are presented.

**Key words:** Entropy generation, bleeding, inclined backward step.

## INTRODUCTION

The optimization and improvement of thermal systems has recently been a topic of great interest due to the relations with the problems of energy conversion, material processing and environmental effects. One of the primary objectives in the design of any energy system is to conserve the useful energy applied to take place in a certain process. The irreversibilities associated within the process components destroy the useful energy and causes to decrease the system performance. The optimal second law design criteria depend on the minimization of entropy generation encountered in fluid and heat transfer processes.

Recently, entropy generation analysis has been extensively applied in many fluid flows with heat transfer in different geometries. Heat transfer and viscous

dissipation are the only sources of entropy generation in force convection fluid flow. Separation flows accompanied with heat transfer are frequently encountered in several engineering application, such as heat exchangers, gas turbine, combustion chamber and ducts used in industrial applications. These types of flow are intrinsically irreversible because of viscous dissipation, separation, reattachment and recirculation. The flow over backward-facing step (BFS) has the most features of separated flows. There are many studies in which the BFS flows were analyzed from a fluid mechanics or a heat transfer perspective. Although, the geometry of BFS flow is very simple, but the heat transfer and fluid flow over this type of step contain most of complexities. Consequently, it has been used in the benchmark investigations. In the benchmark problem, a steady state two-dimensional mixed convection laminar flow in a vertical channel with a BFS was solved numerically. By now, more than ten papers were contributed in which the benchmark problem was solved

\*Corresponding author. E-mail: [ganjali2000@yahoo.com](mailto:ganjali2000@yahoo.com). Tel: 09131407549.

numerically by different methods [Blackwell and Armaly, 1993].

A review of research on laminar mixed convection flow over forward- and backward-facing steps was done by Mulaweh [2003]. Armaly et al. [1983] analyzed laminar, transition, and turbulent isothermal flows over a BFS experimentally. Flow over a BFS with forced convection heat transfer was conducted by other investigators by different numerical techniques [Vradis et al., 1992; Pepper et al., 1992; Vradis and Van Nostrand, 1992; Tylli et al., 2002; Brakely et al., 2002].

In all of the above works, the step was considered to be vertical to the bottom and top walls. It is obvious that there are many engineering applications in which the forward- or backward-facing step is inclined. In a recent study, the first author studied the turbulent forced convection flow adjacent to inclined forward step in a duct [Gandjalikhan et al., 2009]. In that study, the Navier-Stokes and energy equations were solved in the computational domain by CFD method using conformal mapping technique based on the Schwarz-Christoffel transformation. By this method, the effect of step inclined angle on flow and temperature distributions was determined.

Investigation of entropy generation in the flow over BFS has many engineering applications, such as computation of irreversibility and energy loss in separated regions encountered for flow over gas turbine blades where both viscous effect and heat transfer are present. There are a few studies in which the analysis of entropy generation due to forced convective flow over a BFS has been conducted [Abu Nada, 2005, 2006].

On the other hand, the problems of fluid flow in ducts and channels with permeable walls have received much attention from investigators due to increasing use of suction and injection in modern technology. A particularly relevant example is that of turbine blades of the modern aircraft engines, which are currently cooled by the passage of relatively cool air tapped from the compressor, either through hollow blades or through span wise holes drilled in solid blades. The technique of transpiration cooling was demonstrated as early as the late 1948's [Duwez and Mheeler, 1948], and interest has recently been focused upon transpiration-cooled turbine blades. There are several studies in which the fluid flows through ducts and channels with bleeding were studied [Mehta and Jain, 1962; Erdogan and Imrak, 2005]. Recently, investigation of entropy generation in a flow over a right angle BFS under bleeding condition was done by Abu-Nada [2009]. In that work, the set of governing equations were solved by the finite volume method and the distributions of entropy generation number on solid surfaces at different conditions were calculated. Moreover, the effects of bleed coefficient for both blowing and suction on the entropy generation number and Bejan number were presented. Although there are some studies about entropy generation in many process components such as BFS flow, but a careful

inspection of the literature shows that the entropy generation in forced convection flow over inclined BFS under bleeding is still not studied. Therefore, the present research deals with the investigation of entropy generation in a forced convection flow adjacent to inclined BFS in a duct with bleeding effect. Toward this end, the set of governing equations consists of conservation of mass, momentum and energy are solved by CFD method. Because of the complex flow geometry, conformal mapping is used to generate an orthogonal grid and the set of governing equations are transformed to the computational domain by numerical integration of the Schwarz-Christoffel transformation. Discretized forms of the governing equations are obtained by integrating over each control volume in the computational domain and the SIMPLE algorithm is used for pressure-velocity coupling. From the numerical results, the effects of two important factors, those are step angle and bleeding coefficient on the distributions of entropy generation number, Nusselt number, Bejan number and friction coefficient are studied.

## THEORY

To find the entropy generation for the convection flow shown in Figure 1, the fluid velocity and temperature distributions inside the flow domain are calculated by numerical solution of the governing equations. These equations are continuity, momentum and energy including convection and diffusion terms. The fluid flow is considered to be laminar, two-dimensional and incompressible and all thermo-physical properties of fluid are constant. The non-dimensional forms of the governing equations are given as follows:

$$\frac{\partial U}{\partial X} + \frac{\partial V}{\partial Y} = 0 \quad (1)$$

$$\frac{\partial}{\partial X} \left( U^2 - \frac{1}{Re} \frac{\partial U}{\partial X} \right) + \frac{\partial}{\partial Y} \left( UV - \frac{1}{Re} \frac{\partial U}{\partial Y} \right) = - \frac{\partial P}{\partial X} \quad (2)$$

$$\frac{\partial}{\partial X} \left( UV - \frac{1}{Re} \frac{\partial V}{\partial X} \right) + \frac{\partial}{\partial Y} \left( V^2 - \frac{1}{Re} \frac{\partial V}{\partial Y} \right) = - \frac{\partial P}{\partial Y} \quad (3)$$

$$\frac{\partial}{\partial X} \left( U\Theta - \frac{1}{Pe} \frac{\partial \Theta}{\partial X} \right) + \frac{\partial}{\partial Y} \left( V\Theta - \frac{1}{Pe} \frac{\partial \Theta}{\partial Y} \right) = 0 \quad (4)$$

In the above equations, the following dimensionless groups are used:

$$(X, Y) = \left( \frac{x}{D_H}, \frac{y}{D_H} \right), \quad (U, V) = \left( \frac{u}{V_0}, \frac{v}{V_0} \right), \quad P = \frac{p}{\rho V_0^2},$$

$$Pr = \frac{\mu c}{k}, \quad Re = \frac{\rho V_0 D_H}{\mu}, \quad \Theta = \frac{T - T_c}{T_h - T_c}$$

Where Pr and Re are the prandtl and Reynolds numbers, respectively,  $D_H$  is the hydraulic diameter and  $V_0$  is the fluid velocity at duct inlet section.

**Boundary conditions**

Equations 1 to 4 are solved with considering appropriate boundary conditions. For the fluid flow problem, no-slip condition is applied on solid boundaries. According to this criteria, the y-component of fluid velocity on the permeable wall with bleeding is set equal to  $V_w$ , such that the positive and negative values for this velocity denote blowing and suction, respectively. Besides, at the inlet section, slug flow with velocity  $V_0$  is considered and at the outlet section, zero axial gradient for velocity components u and v is employed.

For the thermal problem, the top wall and bottom wall including the step are kept at constant temperature  $T_c$  and  $T_h$ , respectively. Besides, at the inlet section, a uniform temperature  $T_1$  is assumed and zero temperature gradient in axial direction is employed at the outlet section.

**Entropy generation**

In the forced convection process the entropy generation is associated to the heat transfer and to the viscous friction. According to Bejan [1982], the local entropy generation (Ns) in dimensionless form can be determined by the following expression:

$$Ns = \left[ \left( \frac{\partial \Theta}{\partial X} \right)^2 + \left( \frac{\partial \Theta}{\partial Y} \right)^2 \right] + \Psi \left\{ 2 \times \left[ \left( \frac{\partial U}{\partial X} \right)^2 + \left( \frac{\partial V}{\partial Y} \right)^2 \right] + \left[ \left( \frac{\partial U}{\partial Y} \right)^2 + \left( \frac{\partial V}{\partial X} \right)^2 \right] \right\} \quad (5)$$

The following dimensionless quantities are used in the calculation of entropy generation:

$$Ns = \frac{S_{gen} D_H^2}{k \tau^2}, \quad \tau = \frac{T_h - T_c}{T_c}, \quad Br = \frac{\mu V_0^2}{k(T_h - T_c)}, \quad \Psi = \frac{Br}{\tau}$$

where Ns is the entropy generation number,  $S_{gen}$  the volume rate of entropy generation, Br the Brinkman number and tau is the non-dimensional temperature difference.

In Equation (5) for computation of entropy generation number, the first term represents entropy generation due to the heat transfer ( $Ns_{cond}$ ), while the second term represents the entropy generation due to the fluid viscous effect ( $Ns_{visc}$ ). An alternative parameter for irreversibilities distribution is the Bejan number (Be) defined as follows [Bejan, 1982]:

$$Be = \frac{Ns_{cond}}{Ns_{cond} + Ns_{visc}} \quad (6)$$

According to the definition of Bejan number, the irreversibilities due to the viscous effect are dominant when  $Be \leq 1/2$ . When  $Be \geq 1/2$ , the heat transfer irreversibilities dominate the process and if  $Be=0.5$ , the entropy generation due to the viscous effect and heat transfer are equal.

**GRID GENERATION**

As described in the previous sections, because of the complex geometry in the physical domain, the set of governing equations are transformed in the computational domain and are solve numerically in this region. Toward this end, the grid generation in the present work is carried out with the numerical integration of the Schwarz-Christoffel transformation. By this technique, a polygon in the (x,y)-plane, is mapped onto the upper half of ( $\xi-\eta$ )-plane as shown in Figure 2. The relation between the Z-plane as physical domain to the  $\gamma$ -plane as computational domain is as follows [Milne-Thomson, 1960]:

$$\frac{dZ}{d\gamma} = A(\gamma - \xi_1)^{-\alpha_1/\pi} (\gamma - \xi_2)^{-\alpha_2/\pi} \dots (\gamma - \xi_N)^{-\alpha_N/\pi} \quad (7)$$

In Equation 7,  $\alpha$  is the angle of counterclockwise rotation at each apex and N is the number of polygon apices. The points  $\xi_i$  ( $i=1,2,\dots,N$ ) are positions on the real axis in  $\gamma$ -plane, where each of them corresponds to an apex of the polygon in Z-plane. The values of parameters  $\xi_i$  are unknown which will be determined iteratively during the numerical procedure. Also, in Equation 7, A is a complex constant which depends on the geometry of physical domain. According to Riemann theorem [Milne-Thomson, 1960], the positions of three points of  $\xi_i$  on the real axis of computational plane are arbitrary. To find the mapping function ( $\gamma$ ), we integrate the differential Equation (Equation 7). Let us do this for the general case of an N-sided polygon with vertices  $z_1, z_2, \dots, z_N$  at which the exterior angles are  $\alpha_1, \alpha_2, \dots, \alpha_N$ :

$$Z(\gamma) = A \int_{\gamma_0}^{\gamma} \prod_{i=1}^N (\gamma - \xi_i)^{-\alpha_i/\pi} d\gamma + B \quad (8)$$

In Equation 8, B is a complex constant and  $\gamma_0$  is a point on the upper half of computational plane. As noted before, the correct selection of points  $\xi_i$  involves an iterative procedure. The details of this transformation and the related numerical procedure in grid generation are given completely in Sridhar and Davis (1985). By this technique, the relation between physical and computational planes is determined from which the values

**Table 1.** Values of parameters  $A'$ ,  $B'$ ,  $\Gamma_\phi$  and  $S_\phi$  in transformed governing equations.

Equation	$A'$	$B'$	$\phi$	$\Gamma_\phi$	$S_\phi$
Continuity	$u^*$	$v^*$	1	0	0
$\xi$ - Momentum.	$u^*$	$v^*$	$u^*$	1/Re	$\frac{\partial}{\partial \xi}(PY_\eta) + \frac{\partial}{\partial \eta}(PY_\xi)$
$\eta$ - Momentum	$u^*$	$v^*$	$v^*$	1/Re	$-\frac{\partial}{\partial \xi}(PY_\xi) - \frac{\partial}{\partial \eta}(PY_\eta)$
Energy	$u^*$	$v^*$	$\Theta$	1/Pe	0

of metric coefficients which are needed to transform the governing equations into computational domain can be obtained. The transformed form of the governing equations in the computational plane for any dependent variable  $\phi$ , can be written in the following common form:

$$\frac{\partial}{\partial \xi} [JA' \phi - \Gamma_\phi \frac{\partial \phi}{\partial \xi}] + \frac{\partial}{\partial \eta} [JB' \phi - \Gamma_\phi \frac{\partial \phi}{\partial \eta}] = S_\phi \quad (9)$$

in which, J is the Jacobian of transformation,  $J = Y_\xi^2 + Y_\eta^2$ , and the values of parameters  $A'$ ,  $B'$ ,  $\Gamma_\phi$  and  $S_\phi$  are given in Table 1 for continuity, momentum and energy equations.

## METHOD OF SOLUTION

Finite difference forms of the transformed partial differential equations (Equation 9) are obtained by integrating over an elemental cell volume with staggered control volumes for the  $\xi$ - and  $\eta$ - velocity components. The discretized forms of the governing equations are numerically solved by the SIMPLE Algorithm of Patankar and Spalding [1972]. Numerical solutions are obtained iteratively by the line-by-line method such that iterations are terminated when the sum of the absolute residuals is less than  $10^{-4}$  for each equation. Numerical calculations are performed by writing a computer code in FORTRAN. Extensive mesh testing is performed to guarantee grid-independency. Based on this study, the optimum grids with 400 to 500 intervals in the  $\xi$ -direction and 100 to 150 intervals in the  $\eta$ -direction dependent to the flow condition are employed with clustering near the solid boundaries and closed to the domains with sharp gradients in dependent variables.

After calculation of velocity and temperature fields, Equation (5) is used to solve for the entropy generation number at each grid point in the physical domain. Besides, the distributions of Nusselt number and coefficient of friction on the top and bottom walls are calculated by the following equations:

$$Nu = \frac{1}{\Theta_w - \Theta_m} \left( \frac{\partial \Theta}{\partial Y} \right)_{\text{Boundary}} \quad (10)$$

$$C_f = \frac{2}{Re} \left( \frac{\partial U}{\partial Y} \right)_{\text{Boundary}} \quad (11)$$

## Validation of computational results

The numerical solution is validated by comparing the calculated entropy generation for a test case with the theoretical finding by Abu-Nada [2009]. In this test case, a laminar forced convection flow over a vertical backward step in a duct with bleeding on the bottom wall in the region  $0 \leq X \leq 10H$  was analyzed. The variations of entropy generation number  $N_s$  along the bottom wall for two different bleed coefficient are shown in Figure 3 with comparison to that obtained in Abu Nada [2009]. Since, in Abu Nada (2009), the step has right angle, the value of step inclined angle is set equal to  $\pi/2$  in the computation of Figure 3. It is seen that the minimum value of  $N_s$  occurs directly at  $x=0$  at the bottom step corner, where the fluid has no motion. Also, Figure 3 shows that the maximum value of  $N_s$  occurs inside the recirculation zone and then it drops sharply to a very low value at the reattachment point after which  $N_s$  increases and approaches to a constant value far from the step. It is seen from Figure 3 that blowing reduces the value of entropy generation number which is due to the decreased temperature and velocity gradients for the case of blowing. However, according to Figure 3, the general agreement between the present results with the theoretical finding in Abu Nada [2009] is quite good and the values of minimum and maximum entropy generation numbers and their predicted locations are reasonably closed to each other.

## RESULTS AND DISCUSSION

The present research results are presented for air flow adjacent to an inclined forward step in a duct at Reynolds number equal to 400, while the Prandtl number is kept constant at 0.71 to guarantee constant fluid physical properties for moderate and small values of temperature difference ( $T_h - T_c$ ). According to the physical domain shown in Figure 1, the expansion ratio ( $ER = H/h$ ) is set equal to 2. Besides, the values of non-dimensional temperatures for the bottom wall (including the step), top wall and inlet fluid are set equal to 1, 0 and 0.7, respectively. The computed domain in the x-direction has a length of  $L = 30H$ , while the distance between the

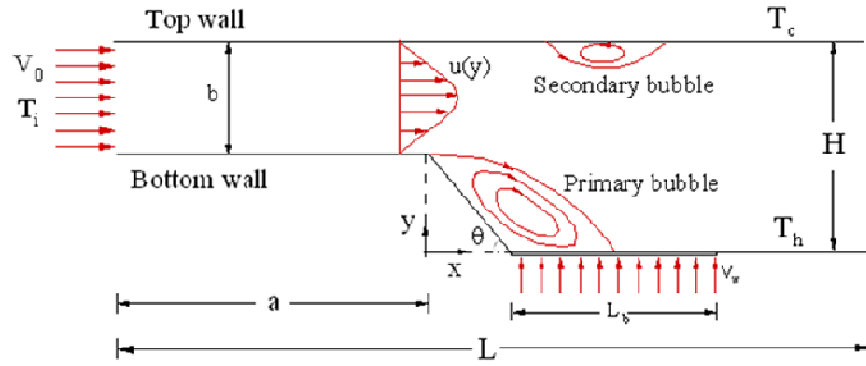


Figure 1. Physical model.

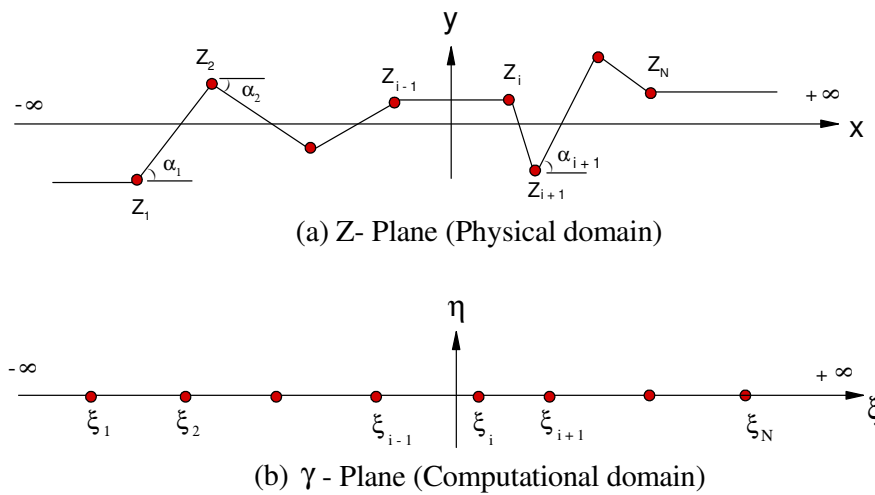


Figure 2. Mapping of a polygon in  $Z(x,y)$ -plane onto the upper half of  $\gamma(\xi-\eta)$  - plane.

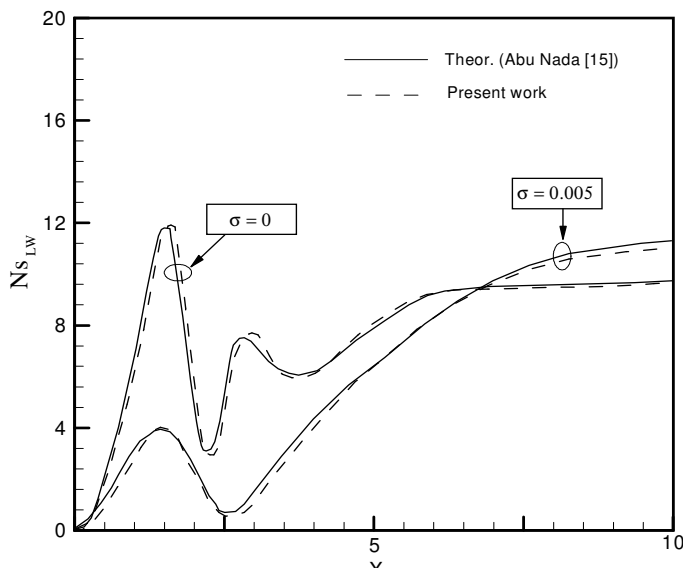
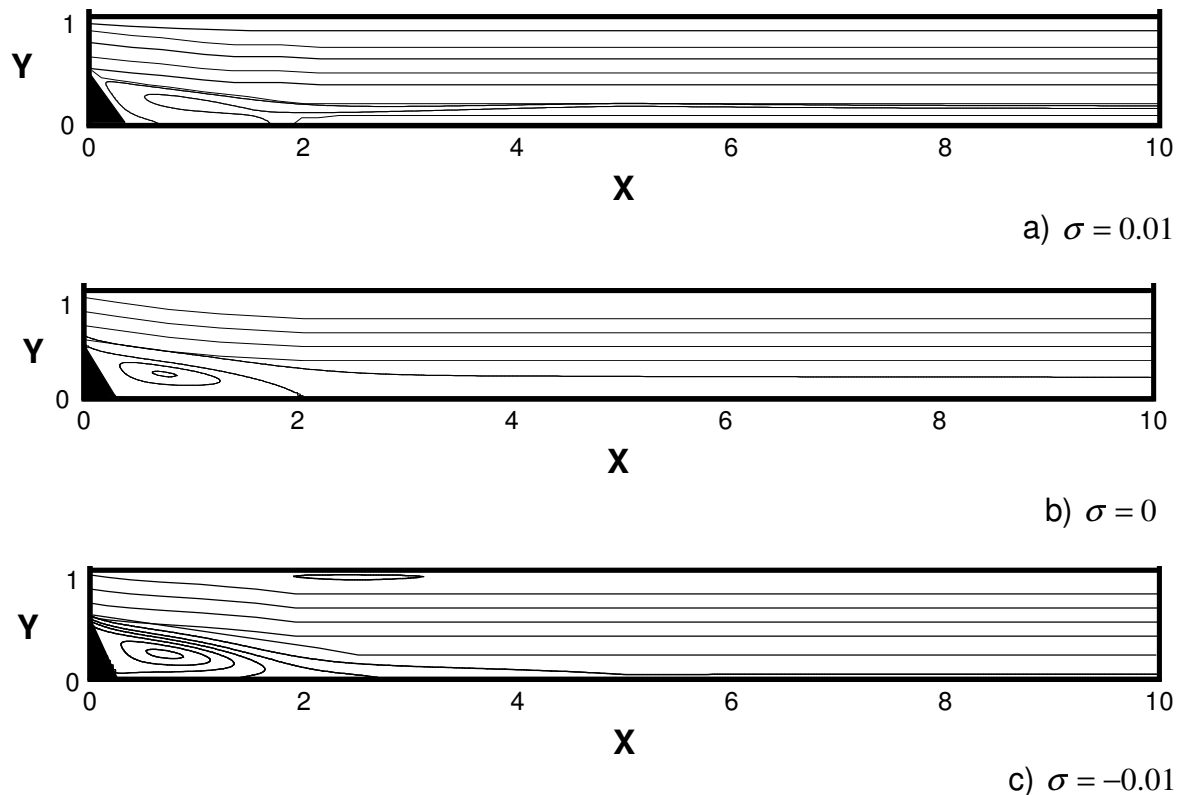


Figure 3. Variation of entropy generation number along the bottom wall  $Re=400$ ,

inlet section and step depicted by  $a$ , is set equal to  $10 H$  to ensure fully developed condition for velocity and temperature distributions before the step. Also in the computations, it is assumed that the permeable wall with bleeding has a length of  $L_b=5 H$  (Figure 1). It is worth mentioning that the values of bleed coefficient used in the present work are  $0$  and  $\pm 0.01$ , where positive and negative values correspond to blowing and suction, respectively, and zero value of bleed coefficient corresponds to impermeable wall.

First in order to show the flow pattern, the streamlines downstream the step are plotted in Figure 4 for an inclined step with  $\theta = 60^\circ$  for three different bleeding coefficient including both suction and blowing. The effect of inclined step on the flow is clearly seen from the curvatures of streamlines. Figure 4 shows a recirculation zone adjacent to the bottom wall downstream the step for all values of the bleeding coefficient. The effect of bleeding on the fluid flow is clearly seen in Figure 4, such that in the case of suction, the secondary recirculation zone also takes place on the top wall after the step. It



**Figure 4.** Streamlines in flow over inclined step in a duct with three different values of bleeding coefficient,  $\theta = 60^\circ$ .

should be noted that for small values of the Reynolds number (say for  $Re < 300$  for this test case), only the primary recirculation zone appears.

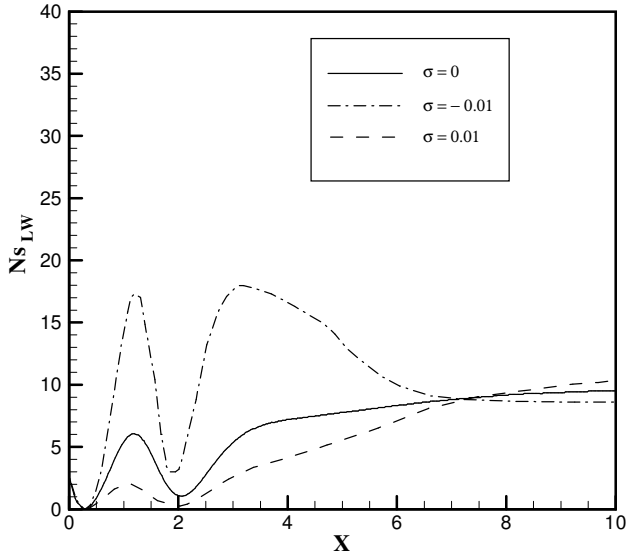
Since, the main task of the present study is to investigate the effect of step inclined angle  $\theta$  and bleeding on the entropy generation and other thermohydrodynamic characteristics of laminar forced convection flow, thereby the following figures are about the effects of these two factors on entropy generation number, Nusselt number, Bejan number and friction coefficient on the solid walls.

Variations of entropy generation number  $N_s$  along the bottom wall for three different values of the bleed coefficient and two different values of the step inclined angle are plotted in Figure 5. It is seen that for all values of bleed coefficient and step inclined angle, the maximum value of  $N_s$  along the bottom wall occurs inside the recirculation zone and then it drops sharply to a very low value at the point of reattachment. This behavior can be explained by noting that after flow separation, the vortices increase dramatically inside the recirculation region that causes to take place maximum value of  $N_s$  in this zone. Besides, at the reattachment point no shear stresses are taking place and the entropy generation is totally due to conduction. It is found in Figure 5 that suction increase the value of  $N_s$  and blowing reduces the entropy generation number. This is related to the increased

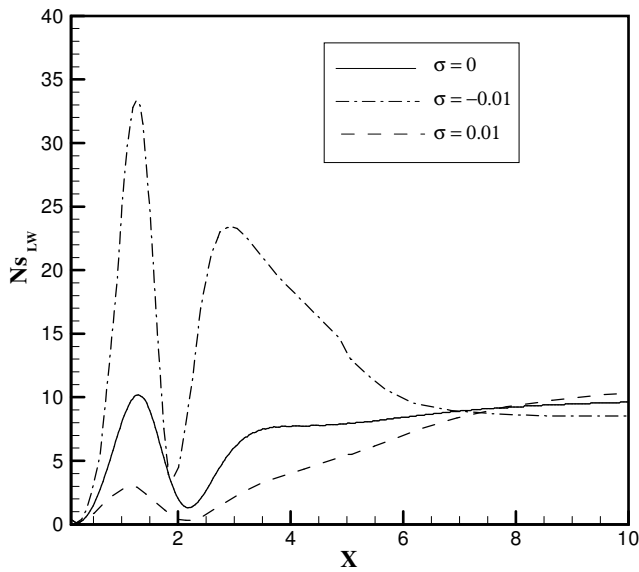
temperature and velocity gradients for the case of suction in comparison to blowing. If one focuses on the entropy generation curves in the vicinity of  $x=0$ , it is seen that  $N_s$  decreases along the projected area of the step and becomes zero on the bottom wall coincides the step corner. Comparison between Figures 5a and b shows that the value of entropy generation number increases with increasing in step inclined angle.

The variations of  $N_s$  along the top wall for the case of right angle step are illustrated in Figure 6. According to this figure, for each value of bleed coefficient, a maximum value for  $N_s$  is detected at  $x=0$ , which is due to the high shear rates encountered due to the development of viscous boundary layer. After the leading edge of top wall, entropy generation number decreases sharply along the wall and the minimum value of  $N_s$  occurs around the point of reattachment. This is related to the fact that the maximum local Nusselt number on the bottom wall coincides with the reattachment point. Besides, Figure 6 presents that the effect of bleed coefficient on  $N_s$  distribution along the top wall is negligible.

For more study about the thermal behavior of convective laminar flow over inclined step, the variations of Nusselt number defined as  $Nu = hD_{\text{H}}/k$  along the bottom wall are plotted in Figure 7. It is seen that the minimum value of  $Nu$  occurs on the bottom wall adjacent to step corner and the maximum value at the reattachment



a)  $\theta = 60^\circ$

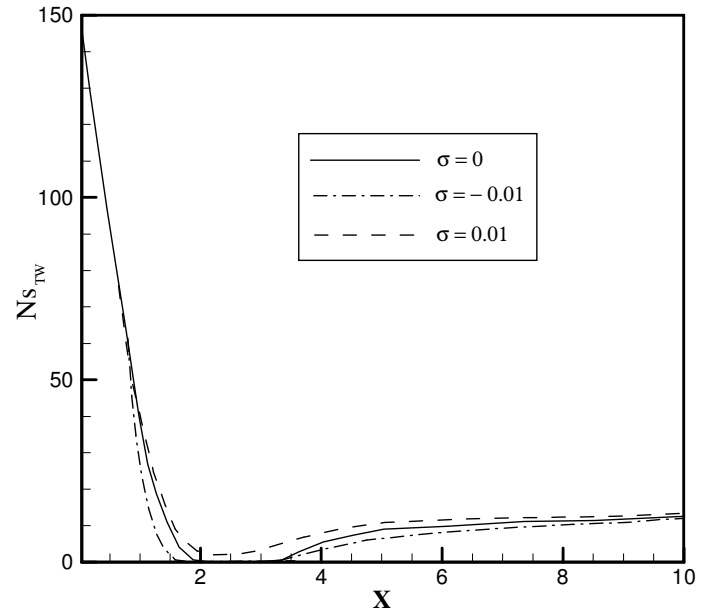


b)  $\theta = 80^\circ$

**Figure 5.** Variation of entropy generation numbers along the bottom wall.

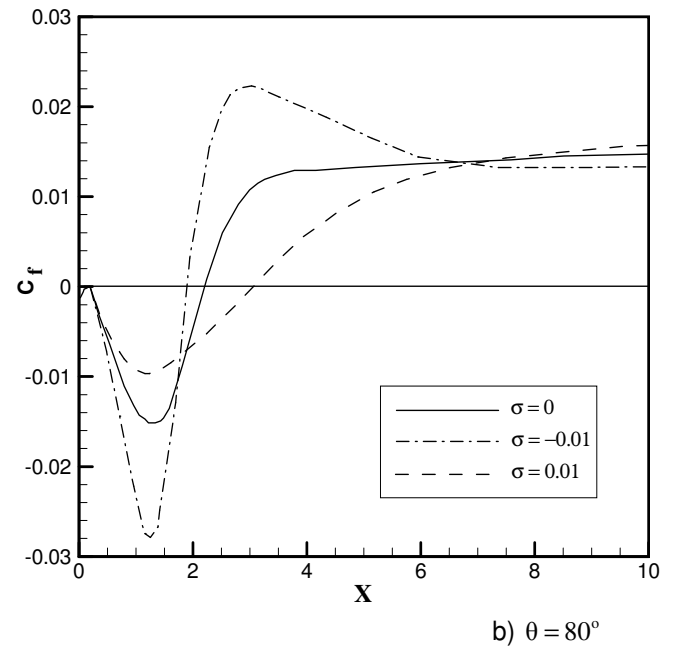
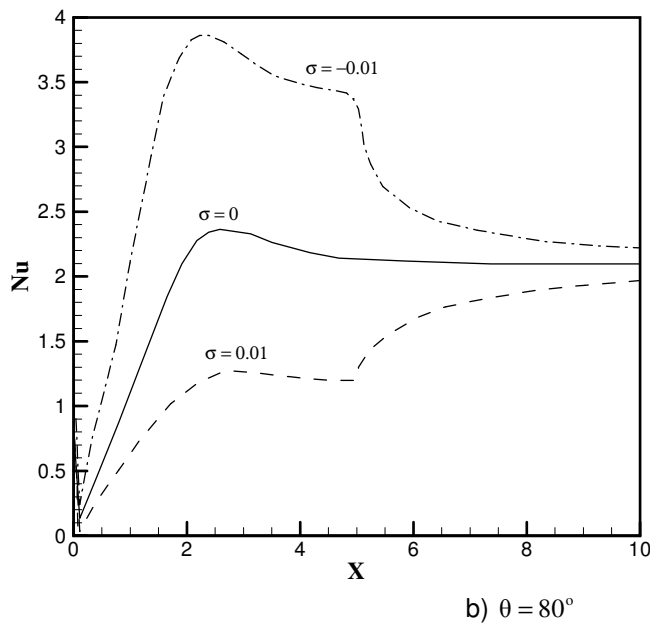
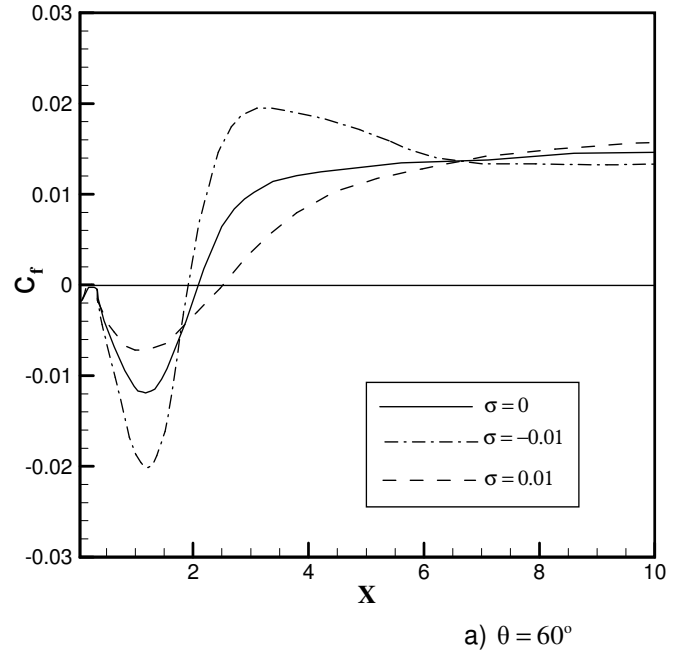
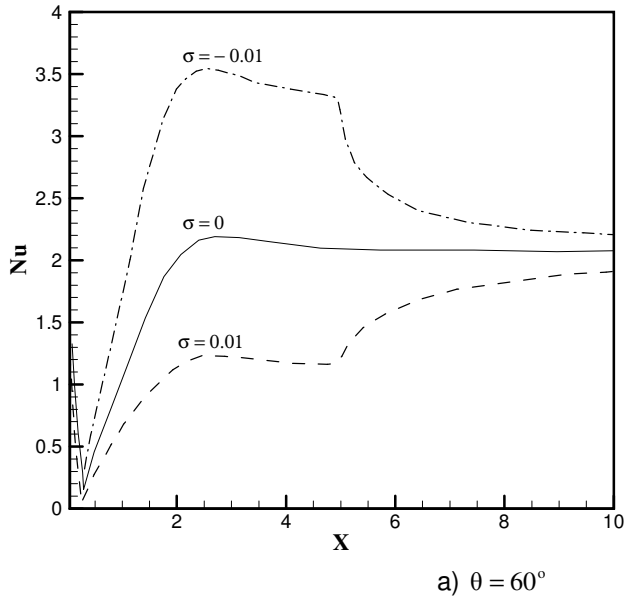
point after which  $Nu$  approaches to a constant value. It is found in Figure 7 that high values of temperature gradients at the bottom wall because of the suction results in higher values of Nusselt number compared to that of blowing. Besides, it can be found that more inclined steps generate high values of convection coefficient on the bottom wall.

Figure 8 presents the distributions of friction coefficient along the bottom wall for various values of bleed coefficient and step inclined angle. It is seen that  $C_f$  is negative inside the circulation zone due to the back flow



**Figure 6.** Variation of entropy generation numbers along the top wall,  $\theta = 90^\circ$ .

and the minimum value of friction coefficient take place in this region after which the value of  $C_f$  becomes equal to zero at the point of reattachment. If one focuses on the  $C_f$  curves for inclined steps in the vicinity of  $x=0$  in detail, it is seen that for inclined steps, the value of friction coefficient is negative along the step projected area and then becomes zero at the step corner on the bottom wall. This is related to this fact that the surface of inclined step is exposed to the back flow which is recognized by the negative values of velocity and negative velocity gradients as shown in Figure 4. By examining the effect of suction on friction coefficient within the recirculation bubble, it is clear that suction increases the absolute value of  $C_f$  which is due to streamlines attraction near to the permeable wall. The effect of blowing on the friction coefficient is opposite to the effect of suction which is due to the repulsion of streamlines from the bottom wall. It is worth mentioning that for the case of suction with negative bleed coefficient, the friction coefficient has a peak value after the reattachment point. This maximum value coincides with the appearance of the secondary recirculation bubble on the top wall. The recirculated region on the top wall narrows down the flow passage and maximized local velocity gradient on the bottom wall. One of another result that can be drawn from Figure 8 for both step inclined dangle is the effect of bleeding on the extent of recirculated zone. It is clear that the extent of domain with negative value for  $C_f$  shows the breadth of recirculated zone. It is seen that in the case of blowing, a wide recirculated domain exists adjacent the bottom wall



**Figure 7.** Variation of Nusselt number along the bottom wall.

**Figure 8.** Variation of friction coefficient along the bottom wall.

in comparison to suction. If one compares the curves plotted in Figures 8a and b, it can be concluded that the absolute value of friction coefficient increases by increasing in the step inclined angle.

Figure 9 presents the variations of Bejan number along the bottom wall under suction, blowing and impermeable wall conditions. As it was mentioned before, the Bejan number is the ratio of entropy generation due to conduction to the total entropy generation. It should be recalled that in all case studies, the upper corner of the step is fixed at the section  $x=0$ . Figure 9 shows that just

after the step, the Bejan number has a great value equal to unity because of zero velocity gradient on the bottom wall at the step corner. Also, the value of  $Be$  becomes equal to unity at the point of reattachment due to zero skin friction coefficient. Also, it can be seen that the minimum values of  $Be$  occur inside the lower primary recirculation zone due to increased value of frictional entropy generation. Comparison between the curves plotted in Figure 9 for three different values of bleed coefficient shows a similar pattern for  $Be$  distributions in

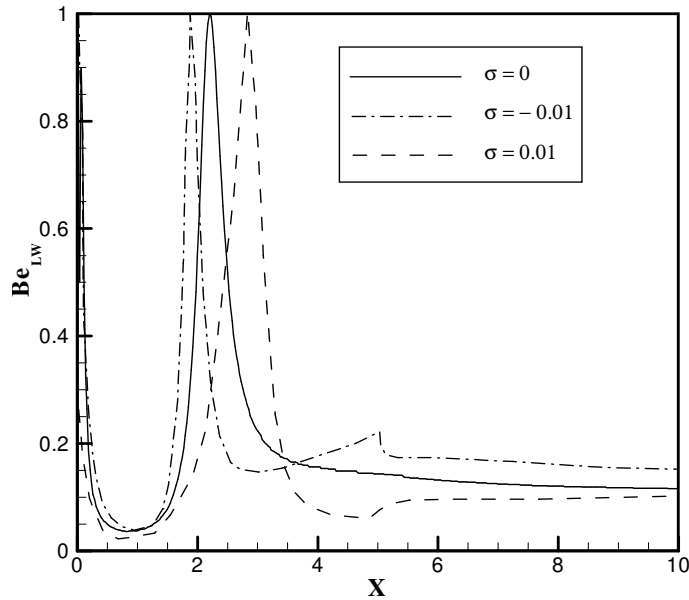


Figure 9. Variation of Bejan number along the bottom wall ( $\theta=90^\circ$ ).

the cases of suction, blowing and impermeable wall. But the location of maximum Bejan number (the reattachment point) moves towards the downstream side by changing the value of bleed coefficient from negative value to zero and then to positive value.

**Conclusion**

Entropy generation in flow over on an inclined backward-facing step is calculated numerically under bleeding condition using suction/blowing. The set of governing equation for the fluid flow, heat transfer and entropy generation are solved numerically by CFD techniques in the computational domain. Because of the complex flow geometry, conformal mapping is used to generate an orthogonal grid by means of the Schwarz-Christoffel transformation. The governing equations are transformed into the computational domain and the discretized forms of the governing equations obtained by the control volume method are solved numerically. By this method, entropy generation due to separation, reattachment, recirculation and heat transfer is studied for flow over inclined step in a duct with bleeding. It was found that the entropy generation is affected by step inclined angle and bleed coefficient such that more irreversibilities take place in flows over steps with high inclined angle under suction.

**NOMENCLATURE**

a: distance between inlet section and step (m)

- b: duct height before the step (m)
- Be: Bejan number
- Br: Brinkman number
- c: heat capacity (kJ/kg K)
- $C_f$ : friction coefficient
- $D_H$ : hydraulic diameter  $=2b$  (m)
- ER: expansion ratio (H/b)
- H: channel height after the step (m)
- h: convection coefficient ( $W.m^{-2}.K^{-1}$ )
- k: thermal conductivity ( $W.m^{-1}.K^{-1}$ )
- L: length of the channel (m)
- $L_b$ : length of permeable wall with bleeding (suction / blowing) (m)
- Ns: entropy generation number
- Nu: Nusselt number
- P: dimensionless pressure
- P: pressure (Pa)
- Pr: Prandtl number
- $S_{gen}^*$ : volume rate of entropy generation ( $W.m^{-3}.K^{-1}$ )
- Re: Reynolds number
- T: temperature (K)
- (u, v): x- and y- velocity components (m / s)
- $(u^*, v^*)$ : velocity components in  $\xi$ -and  $\eta$ -directions
- $V_0$ : fluid velocity at inlet section (m / s)
- (x,y): coordinates in physical plane (m)
- (X, Y): dimensionless forms of (x,y)
- Z: physical plane
- z: a point in physical domain

**Greek symbols**

- $\alpha$ : angle
- $\gamma$ : computational plane
- $(\xi, \eta)$ : coordinates in computational plane
- $\theta$ : step inclined angle
- $\mu$ : dynamic viscosity ( $kg m^{-1}s^{-1}$ )
- $\rho$ : density ( $kg.m^{-3}$ )
- $\sigma$ : bleed coefficient,  $v_w/V_0$
- $\tau$ : dimensionless temperature parameter
- $\Theta$ : non-dimensional temperature
- $\phi$ : dependent variable
- $\Psi$ : viscous dissipation number

**Subscripts**

- c: cold wall
- cond: conduction

h: hot wall  
 i: inlet  
 m: bulk value  
 w: wall  
 visc: viscous

## REFERENCES

- Abu Nada E (2005). Numerical prediction of entropy generation in separated flows. *Entropy*, 7(4): 234-252.
- Abu Nada E (2006). Entropy generation due to heat and fluid flow in backward-facing step flow with various expansion ratios. *Int. J. Energy*, 3(4): 419-435.
- Abu Nada E (2009). Investigation of entropy generation over a backward-facing step under bleeding conditions. *Energy Conversion Manage.*, 49: 3237-3242.
- Armaly BF, Durst F, Pereira JCF, Schonung B (1983). Experimental and theoretical investigation of backward-facing step flow. *J. Fluid Mech.*, 127: 473-496.
- Bejan A (1982). *Entropy generation through heat and fluid flow*, Wiley, New York.
- Blackwell BF, Armaly BF (1993). Computational aspect of heat transfer benchmark problems, in: *ASME Winter Annual Meeting, HTD*, 258: 1-20.
- Brakely D, Gabriela M, Gomes M, Henderson RD (2002). Three-dimensional instability in flow over a backward-facing step. *J. Fluid Mech.*, 473: 167-190.
- Duwez P, Mheeler HL (1948). Experimental study on cooling by injection of fluid through porous material. *J. Inst. Aero. Sci.*, 15: 509-521.
- Erdogan ME, Imrak CE (2005). On the axial flow of an incompressible viscous fluid in a pipe with a porous boundary. *Acta Mech.*, 178: 187-197.
- Gandjalikhan S, Nassab A, Moosavi R, Hosseini-Sarvari SM (2009). Turbulent forced convection flow adjacent to inclined forward step in a duct. *Int. J., Therm. Sci.*, 48: 1319-1326.
- Mehta KN, Jain RK (1962). Laminar hydrodynamic flow in a rectangular channel with porous walls. *Proc. Natl. Inst. Sci. India*, 28: 846-856.
- Milne-Thomson LM (1960) *Theoretical hydrodynamics*, 4<sup>th</sup> Edition, Macmillan, New York.
- Mulaweh HIA (2003). A review of research on laminar mixed convection flow over backward- and forward-facing steps. *Int. J. Therm. Sci.*, 42: 897-909.
- Patankar SV, Spalding BD (1972). A calculation procedure for heat, mass and momentum transfer in three-dimensional parabolic flow. *Int. J. Heat Mass. Transfer*, 15: 1787-1806.
- Pepper DW, Burton KL, Bruenckner FP (1992). Numerical simulation of laminar flow with heat transfer over a backward-facing step. In: *Benchmark problems for heat transfer code*, ASME HTD, 222: 66-80.
- Sridhar KP, Davis RT (1985). A Schwarz-Christoffel Method of Generating Two- Dimensional flow Grids. *J. Fluid. Eng.*, 197: 330-337.
- Tylli N, Kaitksis L, Ineichen B (2002). Side wall effects in flow over backward-facing step: Experiments and numerical solutions. *Phys. Fluids*, 14(1): 13835-3845.
- Vradis G, Van Nostrand L (1992). Laminar coupled flow downstream an asymmetric sudden expansion. *J. Thermophys. Heat Transfer*, 6(2): 288-295.
- Vradis GC, Outgen V, Sanchez J (1992). Heat transfer over a backward-facing step: Solutions to a benchmark. In: *Benchmark problems for heat transfer codes*, ASME HTD, 222: 27-34.